REPORT DOCUMENTATION PAGE

Form Approved
OMB No. 0704-0188

1. AGENCY USE ONLY (Leave blank)	2. REPORT DATE	3. REPORT TYPE AND DATES COVERED
	June 17, 1996	Final Technical, 4/1/96-3/31/96

4. TITLE AND SUBTITLE
Non-Contact Ultrasound Systems for Detection of Fatigue and Corrosion Damage in Aircraft

5. FUNDING NUMBERS
AFOSR Grant
F49620-95-1-0251

6. AUTHOR(S)
Robert E. Green, Jr.

7. PERFORMING ORGANIZATION NAME(S) AND ADDRESS(ES)
Center for Nondestructive Evaluation
The Johns Hopkins University
3400 N. Charles St.
Baltimore, MD 21218-2689

AFOSR-TR-96
0341

9. SPONSORING / MONITORING AGENCY NAME(S) AND ADDRESS(ES)
Air Force Office of Scientific Research ~~(AFMC)~~
110 Duncan Avenue, Suite B115
Bolling AFB, DC 20332-0001

NA

10. SPONSORING / MONITORING AGENCY REPORT NUMBER
95-1-0251

11. SUPPLEMENTARY NOTES

12a. DISTRIBUTION / AVAILABILITY STATEMENT
Approved for public release, distribution unlimited

12b. DISTRIBUTION CODE

13. ABSTRACT *(Maximum 200 words)*
This research has been directed at development and application of non-contact laser, electromagnetic acoustic transducers (EMATs), and air-coupled technology to enhance means for ultrasonic detection of fatigue and corrosion damage in military aircraft structures. The methods which have been investigated include:
(1) laser generation/EMAT detection
(2) laser generation and detection
(3) laser generation/air-coupled detection
(4) air-coupled generation and detection

19960726 048

14. SUBJECT TERMS
ultrasound, lasers, EMATs, aircraft

15. NUMBER OF PAGES
27

16. PRICE CODE
unclassified

17. SECURITY CLASSIFICATION OF REPORT	18. SECURITY CLASSIFICATION OF THIS PAGE	19. SECURITY CLASSIFICATION OF ABSTRACT	20. LIMITATION OF ABSTRAC
unclassified	unclassified	unclassified	U

DISCLAIMER NOTICE

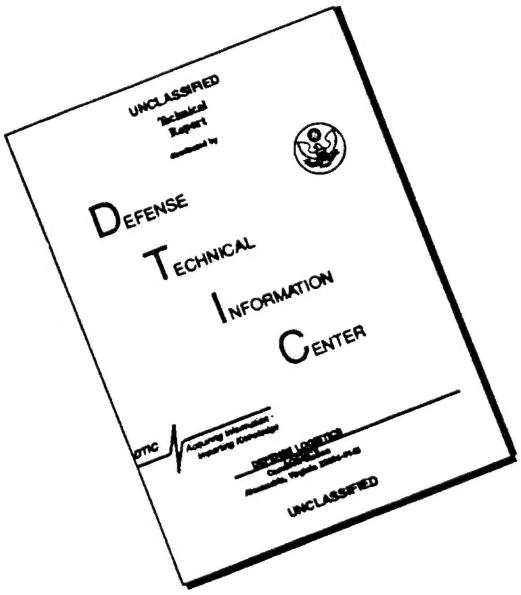

THIS DOCUMENT IS BEST QUALITY AVAILABLE. THE COPY FURNISHED TO DTIC CONTAINED A SIGNIFICANT NUMBER OF PAGES WHICH DO NOT REPRODUCE LEGIBLY.

NON-CONTACT ULTRASOUND SYSTEMS FOR DETECTION OF FATIGUE AND CORROSION DAMAGE IN AIRCRAFT

Robert E. Green, Jr. and James W. Wagner
Center for Nondestructive Evaluation
The Johns Hopkins University
Baltimore, MD 21218-2689

Final Report, June 1996

AFOSR Grant F49620-95-1-0251

ABSTRACT

This research has been directed at development and application of non-contact laser, electromagnetic acoustic transducers (EMATs), and air-coupled technology to enhance means for ultrasonic detection of fatigue and corrosion damage in military aircraft structures. The methods which have been investigated include: (1) laser generation/EMAT detection, (2) laser generation and detection, (3) laser generation/air-coupled detection, (4) air-coupled generation and detection. A completely new design laser generation system capable of generating discrete narrow band frequency ultrasound rather than the broad frequency band ultrasound generated by conventional laser pulses was optimized and applied to EMAT detection of machined slots (simulating cracks) in an aluminum plate. The same new design laser generation system was applied for the experiments involving laser generation and detection of ultrasound. A specially designed laser interferometer was used which has a flat frequency response with virtually no phase shift over the bandpass range of 10 kHz to 10 MHz. This interferometer provided absolute amplitude calibration at the beginning and end of a test as well as instantaneous relative calibration at the moment of measurement. This system was used to examine an actual aluminum aircraft lap joint supplied by Tinker AFB. An optimized air-coupled ultrasound generation and detection system has been developed. The major components of the air-coupled C-scan system are a state-of-the-art ultrasonic measurement system, a high-resolution XYZ-scanning bridge, specially designed air-coupling ultrasonic transducers, and computer control.

BACKGROUND

Since military aircraft of current design are complex, expensive structures and since the present funding situation severely limits the construction of new aircraft, there is an ever increasing demand to assure the longer safe service life of components prior to maintenance disassembly and replacement. Unnecessary time spent on the ground in uneconomical from a financial viewpoint and can be disastrous from a military viewpoint. Therefore, it is imperative that advanced reliable nondestructive evaluation techniques be developed to detect both fatigue and corrosion damage in aircraft currently in service.

Fatigue damage resulting in microcrack and subsequent macrocrack formation constitutes one of the primary mechanisms for loss of structural integrity leading to failure of aircraft components. It has been well documented for all types of fracture that nucleation of cracks in metals occurs as a result of inhomogeneous plastic deformation in microscopic regions. This inhomogeneous plastic deformation can be in the form of slip bands, deformation bands, mechanical twinning, or localized strain concentrations at grain boundaries, precipitates, dispersed particles, and inclusions. Moreover, the mechanisms responsible for these regions of

inhomogeneous plastic deformation are all based on dislocation interactions. In particular, dislocation interactions with point defects, with other dislocations, with stacking faults, with grain boundaries, and with volume defects are known to create regions of severe localized plastic deformation, which develop into microcracks, and these, in turn, either coalesce or grow into macrocracks leading to ultimate fracture.

Therefore, the ideal nondestructive evaluation technique would permit very early detection of fatigue damage so that proper assessment of the severity and rate of severity increase of the structural damage leading to failure can be made. Thus the most sensitive NDE techniques would be capable of detecting motion and pile-up of dislocations; the next most sensitive techniques would be capable of detecting microcracks; the least sensitive systems would be only capable of detecting macrocracks. It is practically expedient to have NDE techniques which can successfully detect fatigue damage in each of these regimes since some components can tolerate larger regions of fatigue damage or larger crack sizes than others without serious concern for the structural integrity of the component.

FATIGUE CRACK DETECTION SURVEY

Historically, nondestructive testing techniques were primarily used to detect the existence of macrocracks in structural materials. Of prime concern in this regard is the size of the smallest flaw which can be detected by each of the nondestructive testing methods. W.D. Rummel et al. (1) conducted a comprehensive statistical analysis of the detectability of artificially induced fatigue cracks in aluminum alloy test specimens. They evaluated 118 test specimens containing a total of 328 fatigue cracks. The cracks ranged in length from 0.018 to 1.27 cm and in depth from 0.003 to 0.451 cm. The test specimens were evaluated in the "as-milled" surface condition, in the "etched" surface condition, and after proof testing, in a randomized inspection sequence. The nondestructive test methods used were x-radiography, dye penetrant, eddy current, and ultrasonics. The 984 nondestructive observations taken using each method served as a sample base for establishment of high confidence levels. Based on the results of their measurements, it was concluded that x-radiography is the least reliable of the four test methods for detection of tight cracks and should not be considered as a sensitive, reliable method for detection of tight cracks. On the other hand, the ultrasonic method was shown to be the most reliable for crack detection as well as to be the most accurate in measuring crack dimensions.

However, the conventional contact ultrasonic techniques can only detect macrocracks and are not able to detect material changes prior to macrocrack formation caused by either fatigue or corrosion damage. The research effort reported here has been directed at development and optimization of several non-contact ultrasonic systems for detection of both fatigue and corrosion damage in aluminum alloy aircraft structures.

ULTRASONIC DETECTION OF FATIGUE DAMAGE

Basically, there are three different ultrasonic techniques which lend themselves to detection of the onset of fatigue damage namely body wave reflection, surface wave reflection, and ultrasonic attenuation.

Body Wave Reflection:

Body wave reflection techniques for fatigue damage detection were first reported in 1964 and have continued to the present time. However, body wave reflection techniques are not sensitive to material changes which give warning of fatigue damage prior to macrocrack formation. The main reason for this is that in order for an easily detectable fraction of the incident ultrasonic energy to be reflected from a crack back to the transducer, the crack must be relatively large, and often the structure will already be well on the wave to fracture.

Surface Wave Reflection:

Although surface wave reflection techniques have been used since 1962 to detect fatigue cracks, they are not sensitive to material changes which give warning of fatigue damage prior to macrocrack formation. The surface condition of the structure and proper transducer attachment are special problems associated with the use of surface waves. Moreover, in many materials internal stress concentrations cause cracks to form in the interior of the structure and not at the surface where they can be detected by surface waves.

Ultrasonic Attenuation:

The first ultrasonic technique used to study the development of fatigue damage during fatigue cycling was the ultrasonic attenuation technique. As early as 1956, R. Truell and A. Hikata (2) observed changes in ultrasonic attenuation in the early stages of fatigue cycling on polycrystalline aluminum specimens. Similar measurements have continued up to the present time (3-32), a large portion of which was sponsored by the Air Force Office of Scientific Research. Although this technique has been proven to be the optimum one to detect early fatigue damage, it has not proven useful for field use because of the problem of acoustically coupling the transducer to the structure in a reproducible fashion.

ULTRASONIC DETECTION OF CORROSION DAMAGE

Although the need to nondestructively detect corrosion damage in military aircraft has been recognized for over 10 years, the fact that many aircraft currently in service are scheduled to fly well past their original design life up to the year 2040, greatly increases the requirement for a reliable nondestructive method to detect corrosion. Recently a number of efforts have been initiated to nondestructively detect corrosion in aluminum alloy aircraft components. However, to the best of the present investigators knowledge, none of these techniques involve ultrasonic attenuation measurements. Since any corrosion product on the surface of aluminum alloys will result in an increase in ultrasonic attenuation, this technique also has a very high probability of detecting even small amounts of hidden corrosion.

CONTACT OR WATER COUPLED TRANSDUCERS

Historically, piezoelectric crystals such as quartz were predominantly used as transducer materials. Currently, poled ferroelectric ceramics are most often used. A major problem associated with conventional ultrasonic techniques is the requirement that the piezoelectric transducers be acoustically bonded to the test material with some sort of acoustical impedance matching coupling medium such as water, oil, or grease; or often more harmful, is the necessity of immersing the entire material structure to be tested in a tank of water or coupling the transducers to the workpiece using water squirter systems. Although the couplant allows acoustical energy to propagate into the test material, it causes several problems in addition to potential harm to the material. For velocity measurements, which are necessary for material thickness measurements, the coupling medium can cause transit time errors on the order of one percent of the measured values. Due to partial transmission and partial reflection of the ultrasonic energy in the couplant layer, there may be a change of shape of the waveform which can further affect velocity measurement accuracy. This can also lead to serious errors in absolute attenuation measurements of up to twenty percent of the measured values. This latter fact is the reason that so few reliable absolute measurements of attenuation are reported in the scientific literature.

It is also important to note that the character of the piezoelectric transducer itself exerts a major influence on the components of the ultrasonic signal, since conventional transducers do not respond as a simple vibrating piston and have their own frequency, amplitude, and directional response. In addition, they "ring" at their resonance frequency and it is extremely difficult to

distinguish between the amplitude excursions caused by this "ringing" and the amplitude variations actually characteristic of the ultrasonic signal. They are also limited in their frequency response and, since they are in contact with the surface of the material to be tested, they can load this surface and thereby modify the ultrasonic wave itself.

NON-CONTACT TRANSDUCERS

A method of non-contact generation and detection of ultrasound is therefore of great practical importance. Several such techniques are presently available in various stages of development, namely capacitive pick-ups, electromagnetic acoustic transducers (EMAT'S), laser beam optical generators and detectors, and more recently air-coupled ultrasonic systems. However, as the name implies, capacitive pick-ups cannot be used as ultrasonic generators and, even when used as detectors, the air gap required between the pick-up and test structure surface is extremely small, which in essence causes the device to be very nearly a contact one.

EMAT's, on the other hand, have been successfully used for material defect characterization particularly in metal bars, tubes, pipes, and plates. One major problem with EMAT's is that the efficiency of ultrasound generation and detection rapidly decreases with lift-off distance between the EMAT'S face and the surface of the test object. They can obviously only be used for examination of electrically conducting materials. Because of the physical processes involved they are much better detectors than generators of ultrasound.

Laser beam ultrasound generation and detection overcomes all of these problems and affords the opportunity to make truly non-contact ultrasonic measurements in both electrically conducting and non-conducting materials, in materials at elevated temperatures, in corrosive and other hostile environments, in geometrically difficult to reach locations, and do all of this at relatively large distances, i.e. meters, from the test object surface (33). Furthermore, lasers are able to produce simultaneously both shear and longitudinal bulk wave modes as well as Raleigh and plate modes.

Air-coupled ultrasonic systems have been recently developed (34-36) and currently research is underway to optimize them for practical non-contact ultrasonic applications. These systems are relatively similar to conventional contact ones and, therefore, when optimized may play an important role in modern nondestructive evaluation of military aircraft.

LASER GENERATION/LASER GENERATION OF ULTRASOUND

Three different mechanisms account for the generation of ultrasonic waves by the impact of pulsed laser beams, namely radiation pressure, ablation, and thermoelasticity (37). Radiation pressure, which is caused by momentum transfer from the incident electromagnetic pulse, is the least efficient of the three proposed mechanisms and is therefore of little importance for practical applications. At the other extreme, when a laser pulse possessing sufficient power density strikes the surface of a material the electromagnetic radiation is absorbed in a very thin layer of the material and vaporizes it. The amplitude of the ultrasonic wave generated in the material by this ablation process can often be increased by placing a coating of a material possessing different thermal properties on the surface of the test object. Although the surface of the test object is slightly damaged when ablation occurs, in certain cases the amount of damage is acceptable when such a generation process is the only way to obtain ultrasonic waves of sufficient amplitude in a non-contact manner. The thermoelastic process consists of absorption of a laser pulse possessing moderate energy in a finite depth of the material under investigation such that thermal expansion causes a volume change and consequently an elastic wave. Thus, the thermoelastic process is the only process which is truly nondestructive and still capable of generating an ultrasonic wave of sufficient amplitude for nondestructive evaluation purposes.

Laser detection of ultrasonic signals is usually performed using an interferometer system to detect the minute displacements of an object surface as the ultrasonic waves impinges upon or propagates along it. A beam of laser light is reflected from the object surface back into the interferometer system so that changes in the optical phase or Doppler shifted frequency can be detected (38). Detection of ultrasonic signals can be recorded with very broad frequency bandwidths in excess of 100 MHz, if necessary, thereby resulting in very high fidelity recording of actual ultrasonic surface displacements. Fundamental calibration based upon the known wavelength of the laser light means that ultrasonic displacements amplitudes can be measured with a high degree of accuracy. Consequently, absolute attenuation measurements can be made independent of couplant materials, transducer resonances, and other variations inherent in conventional piezoelectric transducer systems. In fact, laser interferometer systems have been designed specifically to facilitate highly accurate attenuation measurements of surface and plate waves (39,40).

Although they possess high fidelity and are highly accurate, laser interferometric receivers are the weak link in laser-based ultrasonic systems. Although the laser generator can be a relatively efficient source of ultrasonic signals, a laser interferometric receiver is somewhat less sensitive than its piezoelectric counterpart. For this reason several schemes have been explored to enhance the overall laser ultrasonic system sensitivity. Direct methods for enhancing sensitivity involve the use of very bright (and often quite expensive) lasers for both the generating and receiving sources (41). Preliminary results have shown great promise for other, more sophisticated methods such as laser generation of narrowband, tone burst signals, and the use of spatial arrays (42-49).

ACCOMPLISHMENTS/NEW FINDINGS

Laser Generation/EMAT Detection

A completely new design laser generation system capable of generating discrete narrow band frequency ultrasound rather than the broad frequency band ultrasound generated by conventional laser pulses has been optimized and applied to EMAT detection of machined slots (simulating cracks) in an aluminum plate. This pulsed laser generation/EMAT detection system is still technically non-contact, but because of the EMAT it is not technically remote, i.e. the EMAT needs to be placed in close proximity to the test structure surface. However, the EMAT does have the advantage that it does not require couplants or special surface preparation. Although the EMAT is not an efficient generator of ultrasound, it is an excellent receiver for angled shear waves and, therefore, the pulsed laser/EMAT combination is a near ideal combination for angled shear wave testing without surface contact.

The novelty of this research is that the pulsed laser/EMAT system is employed in a narrow frequency band or resonant configuration. The EMAT is part of a tunable resonant circuit composed of the EMAT coil itself and an adjustable shunt capacitor. To match the frequency response of the tuned EMAT, the new optimized pulsed laser generation system was used and pulsed in rapid succession at the EMAT's resonant frequency. In addition, this system has some other significant advantages. For example, operation of the laser generator in the thermoelastic regime, which is required for strong angled shear wave generation, can only occur at relatively low laser pulse energy densities. Above some energy density threshold, the event becomes ablative, scarring the surface of the test structure. This ablation causes the additional laser energy to be coupled primarily into the normal longitudinal wave (with lambertian directivity) and the Rayleigh wave at the expense of the new shear wave. This energy threshold limits the amount of energy that can be coupled from a single laser pulse into the angled shear wave mode. In the new optimized laser generation system up to ten laser pulses (from separate lasers) at energies below the ablation threshold illuminate, in rapid succession, a single spot on the surface of the test structure. Consequently, the usable shear wave energy in the material is increased over the maximum that a single laser pulse could provide.

Another advantage of the narrowband system stems from the fact that the angle at which the meander line EMAT is most sensitive is proportional to the wavelength, and therefore frequency, of the ultrasonic waves. An angled shear wave arriving at the surface will have a surface wavelength that is greater than the actual wavelength by a factor proportional to the sine of the angle of incidence. When this surface projected wavelength matches twice the EMAT conductor spacing a current is induced in the coil. Such a resonant meander line EMAT was constructed and tested on an aluminum plate 37 mm thick which contained a one third through thickness saw cut.

As shown in Fig. 1a, the pulsed Nd:YAG infrared laser (1.06 micron, delivering approximately 6 mJ in 9 ns), labeled "I.R." in the figure, and EMAT were used side-by-side. By means of a cylindrical lens the laser beam was focused onto a line source running parallel to the conductor lines of the EMAT on the metal's surface. Fig. 1b, shows the received EMAT signal which consists of the average of ten single laser firings. The signal reflected from the cut is seen at 30 microsec. The Rayleigh surface waveform is visible in the first 10 microsec of the trace.

Although in the initial experiment the pulsed laser/EMAT system used only a single laser pulse, it was capable of detecting the one third through thickness opposite side cut. However, to detect real small cracks it was necessary to increase the signal-to-noise ratio of the system. A single laser pulse generates a broad frequency spectrum of ultrasound resulting in a spectral mismatch with the receiving EMAT. Broadening the EMAT spectral bandwidth to match the laser pulse spectrum has several disadvantages including loss of the adjustable angular selectivity and Rayleigh wave signal suppression. Therefore, it was better to modify the spectrum of the laser generated ultrasonic waves by rapidly pulsing the laser source to match the resonance frequency of the EMAT. This had the added advantage of allowing more shear wave energy to be introduced into the metal than could be thermoelastically by a single laser pulse, while operating at power densities below the ablation threshold.

A new optimized ten cavity laser system, shown schematically in Fig. 2, was used to generate the required periodic pulse train. This multi-element laser system was composed of ten Q-switched Nd:YAG cavities with a common power supply and timing electronics. The timing circuit allowed the cavities to be fired with any desired delay. Turning mirrors were used to direct the infrared (I.R.) light pulses through a cylindrical lens to the surface of the test specimen. The arrangement allowed each cavity's pulse to be focused to a line at a fixed distance adjacent to the EMAT on the metal's surface. The photodiode detected output of the multi-cavity system is shown in Fig. 3a, for the case when all ten cavities were pulsed at 500 ns separation. Fig. 3b shows the frequency power spectrum of the photodiode signal for a 2 MHz firing rate.

An aluminum plate with a "penny-shaped" cut was tested to demonstrate the improved sensitivity of the narrowband laser technique. The penny-shaped cut (Fig. 4) was 3 mm deep, 25 mm end-to-end and 0.7 mm wide. In this figure I.R. indicates the spot where all of the laser pulses were incident. Also indicated is the expected reflected path of ultrasound from the penny-shaped cut to the EMAT. The signals detected by the EMAT for the cases of one, three, five and seven laser pulses are also shown. Note that the cut reflected signal became increasingly larger with respect to the background noise as the number of pulses were increased. At the bottom of this figure are the spectra of the EMAT time signals which demonstrate that adding additional pulses increased the frequency content of the pulse repetition rate.

Laser Generation/Laser Detection:

The same new design laser generation system capable of generating discrete narrow band frequency ultrasound was applied for the experiments involving laser generation/laser detection of ultrasound. A specially designed laser interferometer was used which has a flat frequency response with virtually no phase shift over the bandpass range of 10 kHz to 10 MHz. This interferometer provides absolute amplitude calibration at the beginning and end of a test as well as

instantaneous relative calibration at the moment of measurement. Since, in some experiments, the structure under investigation may move or change optical reflectivity, the latter feature is critical in assuring accurate measurements. This system was used to examine an actual aluminum aircraft lap joint supplied by Tinker AFB. A schematic drawing of the experimental arrangement is shown in Fig. 5.

In order to simulate the bonding between layers of an aluminum lap joint as used in aircraft construction, aluminum plates of 1 mm thickness were bonded together with epoxy. The source and detector were on the same side of the plates and their distance of separation was 10 mm. A 12 mJ 2.5 mm diameter single laser pulse was used as a source. The waveforms shown in Fig. 6 represent the evolution of guided plate modes and were very sensitive to the number of bonded plates (i.e. total thickness). Figures 6a,b,c show the waveforms recorded from a single plate, two bonded plates, and three bonded plates, respectively.

Figure 7 shows the theoretical prediction of single pulse laser generated/laser detected guided plate waveforms in 1, 2, and 3 mm thick aluminum plates. Comparison with Fig. 7 shows that the bonded plates of a given total thickness behave in a manner similar to a single plate of the same thickness. This gives an indication of the integrity of the bonded region. Note that the theoretical waveforms are for single plates of various thicknesses and that the effects of a finite bonding layer between the plates have been neglected. Thus some of the differences between Figs. 6 and 7 may be attributed to these effects.

For the actual lap joint specimen, provided by Tinker AFB, the plate waves generated in the single, double, and triple layers were similar, and comparison with the theoretical waveform for a 1.35 mm thick aluminum plate indicates that these waveforms are plate waves propagating on the top most layer of aluminum Fig. 8. This may indicate incomplete bonding between the layers in the specimen used in this investigation.

Both Figs. 9 and 10 indicate through transmission experiments on epicenter in the actual lap joint specimen. For these experiments a 15 mJ 2.0 mm diameter single laser pulse was used as a source. The experimentally recorded J waveform shown in Fig. 9a was recorded from a portion of a single aluminum layer from which the paint was removed and compared with the waveform recorded from a single aluminum layer which was painted Fig. 9b. These figures show the effect of the outer paint covering on the generation of ultrasonic waves by the laser pulse. The light absorption is increased by the paint which in this case may act as a volume absorber. Longitudinal wave generation from such a source is greatly enhanced. One advantage of using a painted specimen over a bare metallic specimen may be that a lower energy laser may be used to generate ultrasound.

Figure 10 shows the high fidelity of the laser ultrasonic signals which could be useful for detection of slight wall thinning due to corrosion. Note that this is a through thickness transmission measurement with source and receiver on opposite sides and such measurements with source and receiver on the same side of the specimen were unsuccessful. This is partially due to the fact for the same side case surface waves or nearfield plate modes are generated as well as a surface skimming longitudinal wave. Thus in some cases the bulk wave arrival may be masked.

These experimental results seem contradictory in some senses. The bulk wave data on the actual lap joint specimen indicates that these waves are propagating through the interfaces, while the plate wave data suggests that they are not. There are two possible explanations for this: (1) The plates are bonded, but not bonded well so that a small amount of the bulk wave energy passes through the interface. (2) There is porosity or small disbonded regions in the interface.

More experiments need to be performed on well documented lap joints before any final conclusions can be made. As is usual in the development of new or improved nondestructive evaluation experiments, the availability of well characterized calibration specimens is lacking. It is hopeful that the Air Force can remedy this situation.

The most recent research effort has been the development of an optical scanning system that provides area inspection capability, identical to that of a conventional water-immersion C-scan system, but using laser generation and detection to permit remote, non-contact, rapid component inspection. This system uses an ultra-stable single longitudinal mode CW Nd:YAG laser operating at 532nm as the receiving laser and a pulsed Nd:YAG at 1064nm as a generation source. The system incorporates a 2-axis galvanometer scanning system with a 2-inch clear aperture to collect light and uses a confocal Fabry-Perot etalon so that rough surfaces may be accommodated. A schematic of the laser-based C-scan system is shown in Fig. 12.

This laser-based C-scan system was used to inspect a 1/2" thick steel plate for wall thinning and weld integrity assessment. The steel plate measured 24" x 30" and had several representative wall thinning defects milled in the back surface. Each milled area measured 2.5" x 2.5" with depths of 1/16" and 1/8". Additionally, a 6" x 30" plate of 1/2" thick steel was welded at right angles to the large plate so that weld integrity could be evaluated. One weld was purposely made bad in comparison with the others. The laser-based C-scan inspection results are shown in Fig. 13. The top portion of the figure shows the images of the 2.5" x 2.5" recesses milled in the back surface of the plate. On the left if the 1/16" deep recess and on the right is the 1/8" deep recess. The recess areas are clearly visible and the wall thickness variations are easily differentiable. The figures in the bottom section of Fig. 13 show that the laser-based C-scan system can also locate and inspect for weld quality. The good weld is in the upper left of the bottom figures and the bad weld is in the center portion of the figures.

Laser Generation/Air-Coupled Detection

This portion of the research effort has been directed at selecting components and assembling the air-coupled ultrasound experimental system. The major components of the air-coupled C-scan system are a state-of-the-art ultrasonic measurement system (RITEC RAM-10000), a high-resolution XYZ-scanning bridge (SONIX), specially designed air-coupling ultrasonic transducers (Harisonic), and a personal computer. Figure 11 shows a schematic drawing of the experimental arrangement. The transmitting transducer, held by a special fixture which is mounted onto the moving element of the scanning bridge, is driven by a computer-controlled high power tone burst gated amplifier (part of RAM-10000). Even though this unit allows for frequencies ranging from below 100 kHz to 20 MHz, the C-scan system is mostly operated in the range around 500 kHz, due to the currently available air-probe transducers. Depending on the focus of these transducers, and/or the specimen thickness, the standoff distance can range from less than 1/8 inch to more than 2 inches. The timing module of the RAM-10000 permits generation of tone bursts with up to 255 cycles per burst, at an internal repetition rate ranging from 0.017 Hz to 10 kHz.

Depending on the geometry of the test specimen, either the through transmitted ultrasonic signal or the transmitted echo of the ultrasonic signal is received by the transmitter itself or a second air-coupled transducer behind the specimen. The transmitter-receiver holding fixture allows both transducers to be manually positioned in x,y,z and at an angle to each other, in addition, and independently of the XYZ-scanning bridge. A typical transmitter-receiver holding fixture through transmission setup consists of two 1 inch diameter transducers, both with a 2 inch focus (HAP-00516), where the transmitter is driven by a 504 kHz, 7 cycle long burst, at a repetition rate of 50 Hz.

The electrical signal, produced by the receiving transducer, is fed directly into a low-noise broad-band preamplifier (40-60 dB gain), filtered, and then fed back into the broad-band receiver unit of the RAM-10000, which has an adjustable gain of up to 100 dB. The then following tracking superheterodyne receiver, quadrature phase sensitive detectors, and gated integrators with variable time constant, integrator gate position and width, make it possible to measure and track signals even under extremely noisy conditions. The amplitude and phase data is thereby obtained indirectly via software in the computer from the digitized outputs of the two phase sensitive detectors. This scheme provides an additional real-time digital signal processing capability, such as measurement averaging, or a spectrum analysis when the system is operated in the frequency sweep mode. The received waveform can also be digitized directly and analyzed via the digitizing storage oscilloscope (LeCroy 9410).

The software for the air-coupled C-scan system gives the user complete control over the ultrasonic measurement system, the XYZ-scanning bridge, and the oscilloscope. The scanning bridge has a mechanized resolution of about 6 microns (0.00024 in.) along all three axes, and provides a free travel range of 26 x 22 x 12 inches. However, the actual resolution of the system is primarily determined by the choice of the transducers and the frequency of operation. Thus, when using the above mentioned set of 500 kHz, 2 inch focused transducers, the achieved lateral resolution is typically about 0.5 mm (0.02 in.). All effort has been directed to selecting components and assembling the air-coupled ultrasound experimental system.

Summary:

Among the limited number of non-contact nondestructive evaluation techniques ultrasonics plays a prominent role. Progress has been made in development of non-contact ultrasonic techniques superior to anything developed previously and continuation of this research will lead to a new generation of practical devices for in-service inspection applications. This research is highly relevant to the Air Force mission of ensuring the safe, reliable in-service life of military aircraft especially if flown well past their original design life.

REFERENCES

1. W.D. Rummell, P.H. Todd, Jr., R.A. Rathke, and W.L. Castner, "The Detection of Fatigue Cracks by Nondestructive Test Methods",Materials Evaluation 32, 205-212 (1974).

2. R. Truell and A. Hikata, "Fatigue in 2S Aluminum as Observed by Ultrasonic Attenuation Methods", Watertown Arsenal Technical Report No. WAL 143/14-47 (1956).

3. Narayan R. Joshi and Robert E. Green, Jr., "Ultrasonic Detection of Fatigue Damage", Proceedings of the Symposium on Fracture and Fatigue, George Washington Univ., May 1972, J. Engr. Fract. Mech. 4, 577 (1972).

4. Robert E. Green, Jr., "Ultrasonic Attenuation Detection of Fatigue Damage", Proceedings of the Ultrasonic International 1973 Conference, Imperial College, London, March 1973, p.187, IPC Science and Technology Press, Ltd., Guildford, England (1973).

5. Robert E. Green, Jr. and Robert B. Pond, Sr., "An Ultrasonic Technique for Detection of the Onset of Fatigue Damage", Air Force Office of Scientific Research Final Report AFOSR-TR-76-0811 (1976).

6. John C. Duke, Jr. and Robert E. Green, Jr., "Simultaneous Acoustic Emission and Ultrasonic Attenuation Monitoring of the Mechanical Deformation of Aluminum", Proceedings of the Second International Conference on Mechanical Behavior of Materials, Boston, Massachusetts, p.1646, (August 1976).

7. Robert E. Green, Jr. and Robert B. Pond, Sr., "Ultrasonic Detection of Fatigue Damage in Aircraft Components", First Annual Report (1976-77) Air Force Office of Scientific Research, AFOSR-TR-77-0658 (1977).

8. Robert E. Green, Jr., and Robert B. Pond, Sr., "Ultrasonic and Acoustic Detection of Fatigue Damage", Second Annual Report (1977-78) Air Force Office of Scientific Research, AFOSR-TR-77-0658 (1978).

9. John C. Duke, Jr. and Robert E. Green, Jr., "Capability of Determining Fatigue Mechanisms in 7075 Aluminum by Combining Ultrasonic Attenuation and Acoustic Emission Monitoring", Proceedings of ARPA/AFML Review of Progress in Quantitative NDE Meeting, La Jolla, CA (July 1978), AFML-TR-78-205 (January 1979).

10. Robert E. Green, Jr., "Non-Destructive Methods for the Early Detection of Fatigue Damage in Aircraft Components", Proceedings of AGARD/NATO Lecture Series No. 103 Non-Destructive Inspection Methods for Propulsions Systems and Components, London, England and Milan, Italy (April 1979), AGARD-LS-103, Paper No. 6 (1979).

11. Robert E. Green, Jr. and John C. Duke, Jr., "Ultrasonic and Acoustic Emission Detection of Fatigue Damage", International Advances in Nondestructive Testing, 6, 125-177, Gordon & Breach, NY (1979).

12. John C. Duke, Jr., and Robert E. Green, Jr., "Simultaneous Monitoring of Acoustic Emission and Ultrasonic Attenuation During Fatigue of 7075 Aluminum", International J. Fatigue 1, pp. 125-132 (1979).

13. S.R. Buxbaum, C.L. Friant, S.E. Fick, and R.E. Green, Jr., "Ultrasonic and Acoustic Emission Detection of Fatigue Damage", Annual Report (1978-79), Air Force Office of Scientific Research AFOSR-TR-79-1287 (1979).

14. Richard B. Mignogna, John C. Duke, Jr. and Robert E. Green, Jr., "Early Detection of Fatigue Cracks in Aircraft Aluminum Alloy Sheets", Materials Evaluation 38, pp. 37-42 (1980).

15. S.R. Buxbaum, C.L. Friant, S.E. Fick, and R.E. Green, Jr., "Ultrasonic and Acoustic Emission Detection of Fatigue Damage", Final Report (1976-1980) Air Force Office of Scientific Research AFOSR-TR-80-1069 (1980).

16. Green, Robert E., Jr., "Effect of Metallic Microstructure on Ultrasonic Attenuation", Nondestructive Evaluation: MicrostructuralCharacterization and Reliability Strategies, Otto Buck and Stanley M. Wolf (eds.), Metallurgical Society of AIME, Warrendale, Pa, pp. 115-132 (1981).

17. Mignogna, R.B. and Green, R.E., Jr., "Effects of High Frequency Loading on Materials", Ultrasonic Fatigue, J.M. Wells, O. Buck, L.D. Roth and J.K. Tien (eds.), Metallurgical Society of AIME, Warrendale, PA, pp. 63-85 (1982).

18. Sirian, Charles, R., Conn, Andrew F., Mignogna, Richard B., and Green, Robert E., Jr., "Method of Measuring Elastic Strain Distribution in Specimens Used for High Frequency Fatigue Testing", Ultrasonic Fatigue, J.M. Wells, O. Buck, L.D. Roth and J.K. Tien (eds.), etallurgical Society of AIME, Warrendale, PA. pp. 87-102 (1982).

19. Green, Robert E., Jr., "No destructive Acoustic Testing for Fatigue Damage", McGraw-Hill Yearbook, of Science & Technology 1985 McGraw-Hill Book Co., New York, pp. 291-294 (1984).

20. Green, Robert E., Jr.,"Ultrasonic Attenuation Nondestructive Evaluation of Materials", Proceedings of Eighth International Conference on Internal Friction and Ultrasonic Attenuation in Solids, Urbana, Illinois Journal de Physique 46, C10-827-C10-834 (1985).

21. Green, Robert E., Jr., "Ultrasonic Materials Characterization", Proceedings of Ultrasonics International 85 Conference, London, England, Butterworth, Guildford, England, pp. 11-16 (1985).

22. Green, Robert E., Jr., "Ultrasonic Nondestructive Evaluation", Encyclopedia of Materials Science and Engineering, M.B. Bever (ed.), M.I.T. Press, Cambridge, Massachusetts, pp. 5178-5182 (1986).

23. Green, Robert E., Jr., "Nondestructive Materials Characterization", Proceedings of 31st Army Sagamore Materials Research Conference, Materials Characterization for Systems Performance and Reliability, J.W. McCauley and V. Weiss (Editors), Plenum Press, N.Y., pp. 31-58 (1986).

24. Green, Robert E., Jr., "Ultrasonic Nondestructive Materials Characterization", Proceedings of Analytical Ultrasonics in Materials Research and Testing Conference, NASA Lewis Research Center, Cleveland, Ohio pp. 1-30 (1986).

25. Green, Robert E., Jr., "Ultrasonic Methods", Proceedings of Third Advanced Materials Workshop, Michigan State University, Traverse City, Michigan, September (1986).

26. Green, Robert E., Jr., "Nondestructive Characterization of Materials Properties", Mechanical Engineering, pp. 66-70 (September, 1987).

27. Green, Robert E., Jr., "Some Innovative Techniques for Nondestructive Evaluation of Materials", Novel NDE Methods for Materials, Bhakta B. Rath (ed.), The Metallurgical Society of AIME, Warrendale, PA, pp. 131-139 (1983).

28. Green, Robert, E., Jr., "Nondestructive Evaluation Techniques in Materials Science", in New Materials and Processes, I.L.H. Hansson and H. Lilholt (Eds.), Proceedings of the 5th Scandinavian Symposium on Materials Science, Danish Society for Materials Testing and Research, Ingenhiorhuset, Copenhagen, Denmark, pp. 1-16, (1989).

29. Green, Robert, E., Jr., "Nondestructive Characterization of Materials", Advanced Materials & Processes, ASM International, Metals Park, Ohio, 136, 20-22 (1989).

30. Green, R.E., Jr., Nondestructive Evaluation of Materials, Annual Review of Materials Science 20, 197-217 (1990).

31. Green, R.E., Jr., "Overview of Acoustical Technology for Nondestructive Evaluation", Proceedings of Second International Congress on Recent Developments in Air- and Structure-Borne Sound and Vibration", M.J. Crocker & P.K. Raju (Eds.), Vol. 2, pp. 879-886 (1992).

32. Green, R.E., Jr., "Practical Applications of Nondestructive Materials Characterization", J. Minerals, Metals & Materials, 44, 12-16 (1992).

33. C.B. Scruby and L.E. Drain, Laser Ultrasonics: Techniques and Applications, Adam Hilger, Bristol, UK (1990).

34. Murray, A., Boltz, E., Fortunko, C.M., Mecklenburg, M.F., and Green, R.E., Jr., "Air-Coupled Ultrasonic System for Nondestructive Evaluation of Wooden Panel Paintings", 3rd International Conference on Non-Destructive Testing, Microanalytical Methods and Environmental, American Ceramic Society, Vol. 75, pp. 2225-2231 (1992).

35. Murray, A., Green, R.E., Jr., Boltz, E.S., Renken, M., Fortunko, C.M., and Mecklenburg, M.F., "Air-Coupled Ultrasonic System for Characterizing the Structural Stability of Wooden Panel Paintings", to be published in Nondestructive Characterization of Materials VI, R.E. Green, Jr., K.J. Kozaczek, and C.O. Ruud (Eds.) Plenum Publishing Corp., New York (1994).

36. Alison Murray, Ph.D. Dissertation, Materials Science & Engineering Department, The Johns Hopkins University, Baltimore, MD 21218 (1993).

37. Hutchins, D.A., "Ultrasonic Generation by Pulsed Lasers", Physical Acoustics, Vol. 18, pp. 21-123 (1988).

38. Wagner, J.W., Optical Detection of Ultrasound, Physical Acoustics, Vol. 19, pp. 201-266 (1990).

39. Spicer, J.B. and Wagner, J.W., "Fiber-Optic Based Interferometer for Noncontact Ultrasonic Determination of Acoustic Velocity and Attenuation in Materials", Nondestructive Characterization of Materials, Proceedings of 3rd International Symposium on Nondestructive Characterization of Materials, Saarbrucken, Germany (October 1988), P. Holler et al. Eds., Springer-Verlag, New York, pp. 691-698 (1989).

40. McKie, A.D.W., Wagner, J.W., Spicer, J.B., and Deaton, J.B., "A Dual-Beam Interferometer for the Accurate Determination of Surface Wave Velocity", Applied Optics 30, 4034-4039 (1991).

41. Wagner, J.W. and Spicer, J.B., "Theoretical Noise-Limited Sensitivity of Classical Interferometry", J. Optical Society America B, 4, 1316-1326 (1987).

42. Wagner, J.W., McKie, A.D.W., Spicer, J.B. and Deaton, J.B., "Modulated Laser Array Sources for Generation of Narrowband and Directed Ultrasound", J. Nondestructive Evaluation 9, 263-270 (1990).

43. Deaton, J.B., McKie, A.D.W., Spicer, J.B., and Wagner, J.W., "Generation of Narrow-Band Ultrasound with a Long Cavity Mode-Locked Nd:YAG Laser", Appl. Phys. Lett. 56, 2390-2392 (1990).

44. Deaton, J.B. and Wagner, J.W., "Variable Length Mode-Locked Nd:YAG Laser for Noncontact Generation and Spectral Control of Narrow-Band Ultrasound", Applied Optics 33(6), 1051-1058 (1994).

45. Deaton, J.B. and Wagner, J.W., "Wiener Filtering of Laser-generated Multiple-pulse Narrow-band Ultrasound for Enhanced Detectability by a Laser Interferometer, Ultrasonics 32(3), 187-193 (1994).

46. Murray, T.W. and Wagner, J.W., "Progress in Pulsed Laser Array Techniques for Generation of Acoustic Waves", Review of Progress in QNDE, Vol. 13, 533-539 (1994).

47. Steckenrider, J.S., Murray, T.W., Wagner, J.W. and Deaton, J.B., Jr., "Sensivity Enhancement in Laser Ultrasonics Using a Versatile Laser Array System", J. Acoust. Soc. Am. 97(1), 273-279 (1995).

48. Oursler and Wagner, J.W., "Narrow-band hybrid pulsed laser/EMAT system for non-contact ultrasonic inspection using angled shear waves", Materials Evaluation 53(5), 593-597 (1995).

49. Murray, T.W., Deaton, J.B., and Wagner, J.W., "Experimental evaluation of enhanced generation of ultrasonic waves using an array of laser sources", Ultrasonics 34 (1), 69-77 (1996).

FIGURE CAPTIONS:

Figure 1. (a) Schematic diagram of single laser pulse excitation and EMAT detection of ultrasound in an aluminum plate with a one third through thickness cut simulating a crack.

(b) The crack (cut) reflected signal shown at 30 microseconds.

Figure 2. Schematic diagram of ten cavity Nd:YAG laser system for generation of narrow frequency band ultrasound and EMAT detection.

Figure 3. (a) The photodiode detected output from the ten cavity laser system for the case when all ten cavities were pulsed at 500 nsec separation.
(b) Frequency power spectrum of the photodiode signal for a 2 MHz firing rate.

Figure 4. Multiple pulse laser excitation on ultrasound in an aluminum plate containing a penny shaped cut. The received EMAT signals are shown for one, three, five, and seven pulse sequences. The signal's normalized frequency spectrum is also shown.

Figure 5. Schematic diagram of ten cavity Nd:YAG laser system for generation of narrow frequency band ultrasound and laser interferometer detection.

Figure 6. Experimental waveforms received from single pulse laser excitation of ultrasound in an aluminum lap joint made from 1 mm thick plates bonded with epoxy.

(a) waveform from a single plate
(b) waveform from two bonded plates
(c) waveform from three bonded plates

Figure 7. Theoretically predicted waveforms for single pulse laser generated/laser detected guided plate waveforms in 1, 2, and 3 mm thick aluminum plates. Effects of a finite bonding layer between plates have been neglected.

Figure 8. Laser generated/laser detected plate waves in actual aircraft lap joint specimen. Comparison with theoretical waveforms for a 1.35 mm thick aluminum plate indicates these waveforms are plate waves propagating in the top most layer of aluminum, possibly indicating incomplete bonding between layers.

Figure 9. (a) Experimental single laser pulse generated/laser detected through transmission waveform recorded from a portion of an actual aircraft lap joint single aluminum layer from which the paint was removed.

(b) Experimental single laser pulse generated/laser detected through transmission waveform recorded from a portion of an actual aircraft lap joint single aluminum layer which was painted.

Figure 10. (a) Experimental single laser pulse generated/laser detected through thickness transmission measurement through a single layer of a painted actual aircraft lap joint single aluminum layer.

(b) Experimental single laser pulse generated/laser detected through thickness transmission measurement through a triple bonded layer of a painted actual aircraft aluminum lap joint.

Figure 11. Schematic drawing of the experimental arrangement for laser generation/air-coupled detection of ultrasound.

Figure 12. Schematic laser-based C-scan system.

Figure 13. Laser-based C-scan of 0.5" thick steel plate showing the following images:

Top: 2.5"x2.5" recesses milled in back surface (left 1/16", right 1/8").
Bottom: 1/2" thick welds on back surface (left bad weld, right good weld).

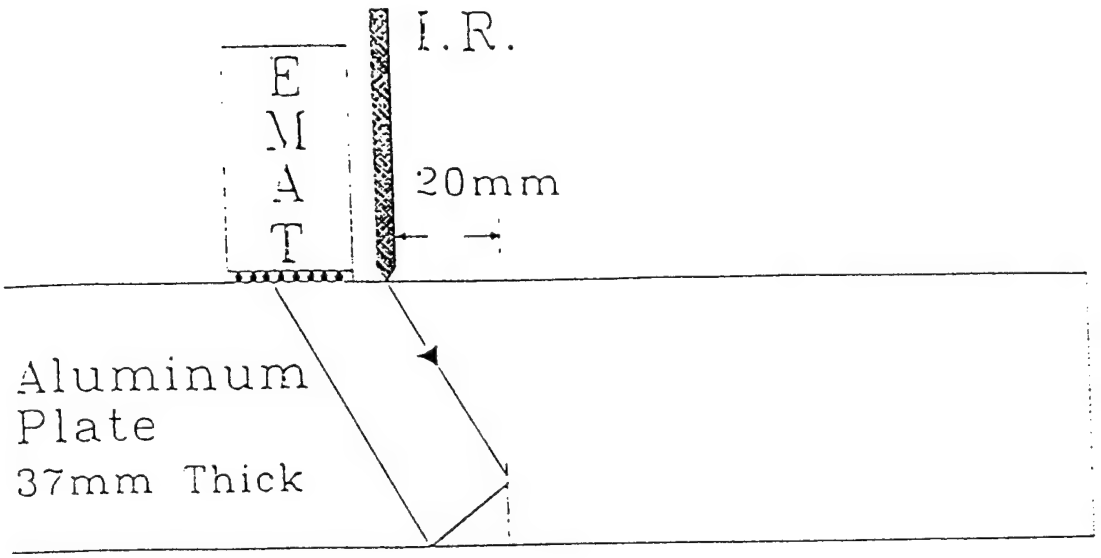

FIGURE 1. (a) Schematic diagram of single laser pulse excitation and EMAT detection of ultrasound in an aluminum plate with a one third through thickness cut simulating a crack.

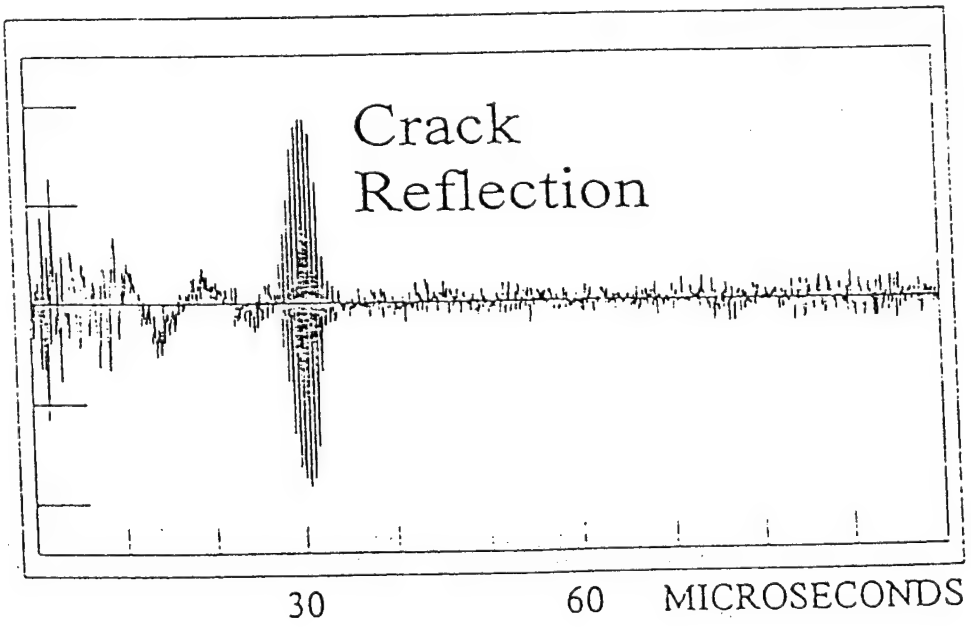

FIGURE 1. (b) The crack (cut) reflected signal shown at 30 microseconds.

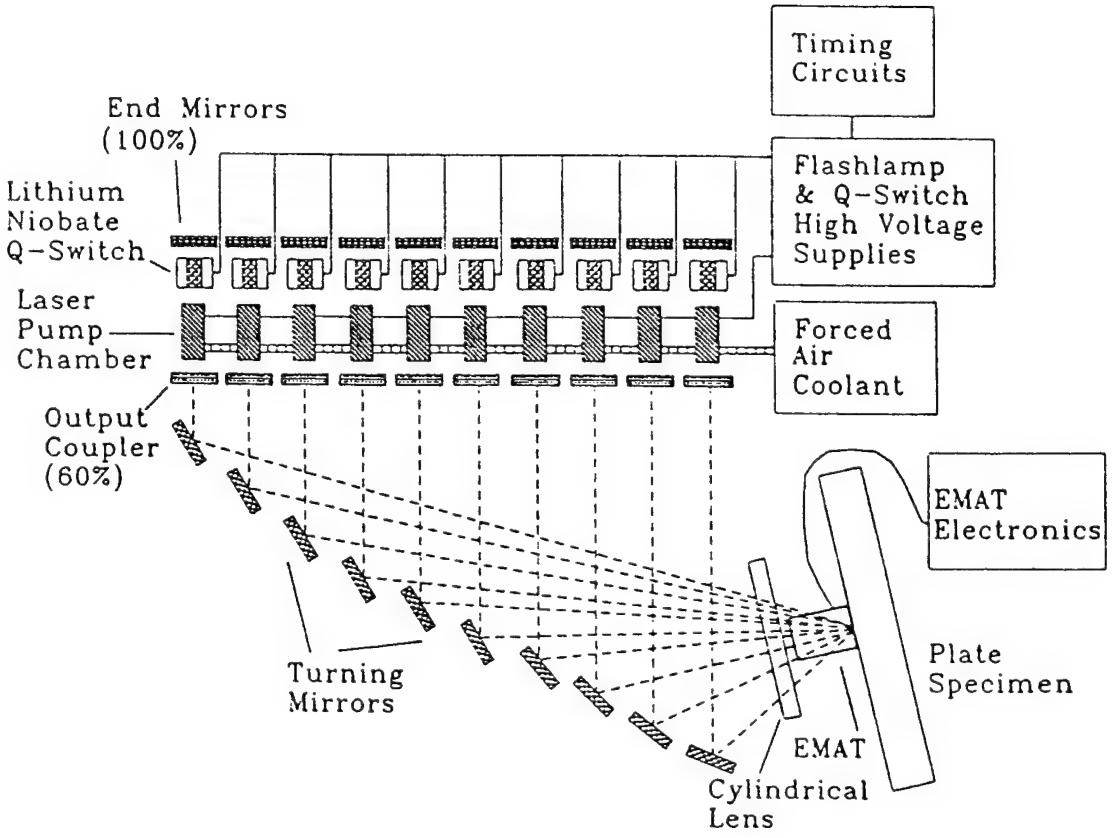

FIGURE 2. Schematic Diagram of ten cavity Nd:YAG laser system for generation of narrow frequency band ultrasound and EMAT detection.

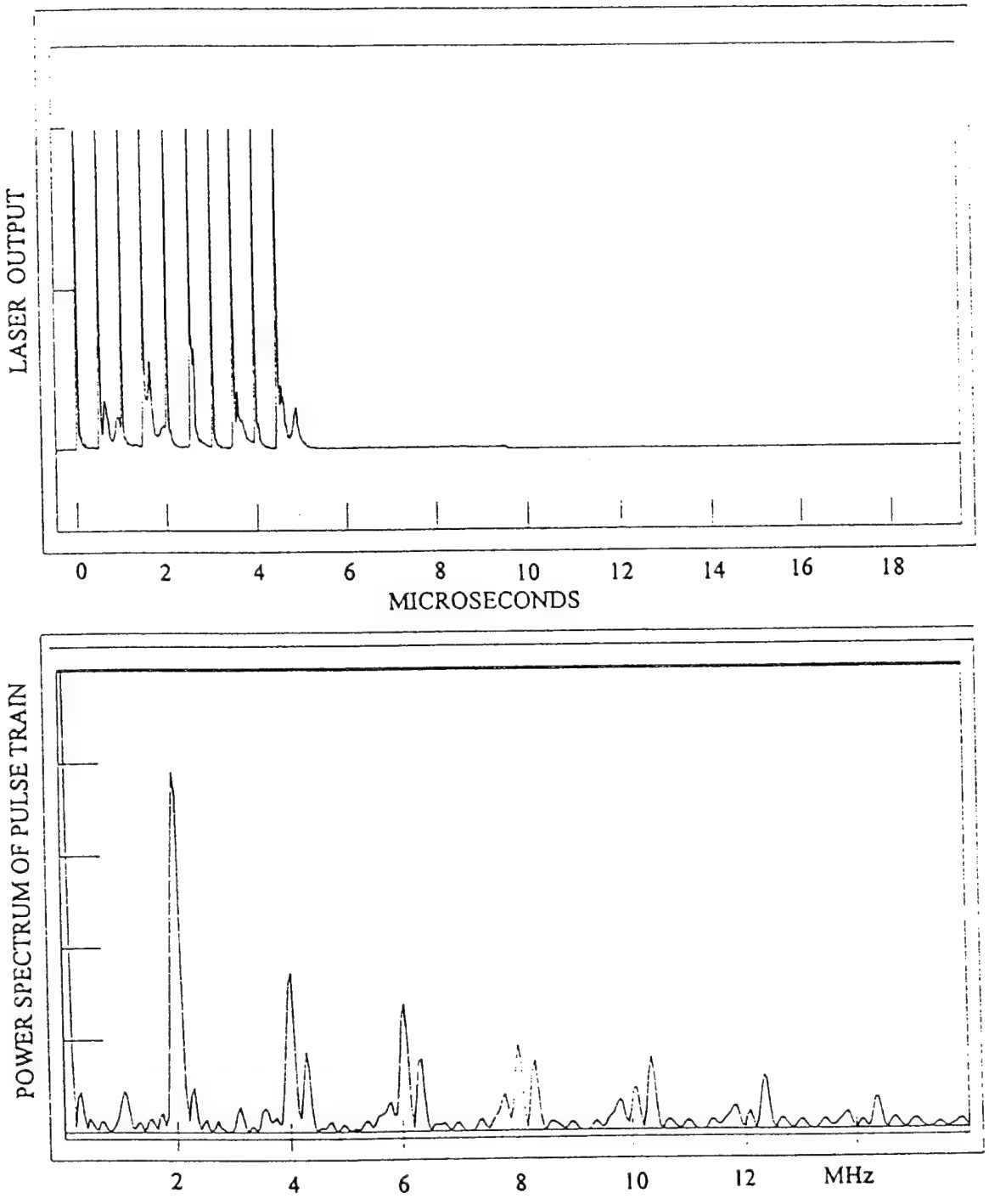

FIGURE 3. (a) The photodiode detected output from the ten cavity laser system for the case when all ten cavities were pulsed at 500 nsec separation.
(b) Frequency power spectrum of the photodiode signal for a 2 MHz firing rate.

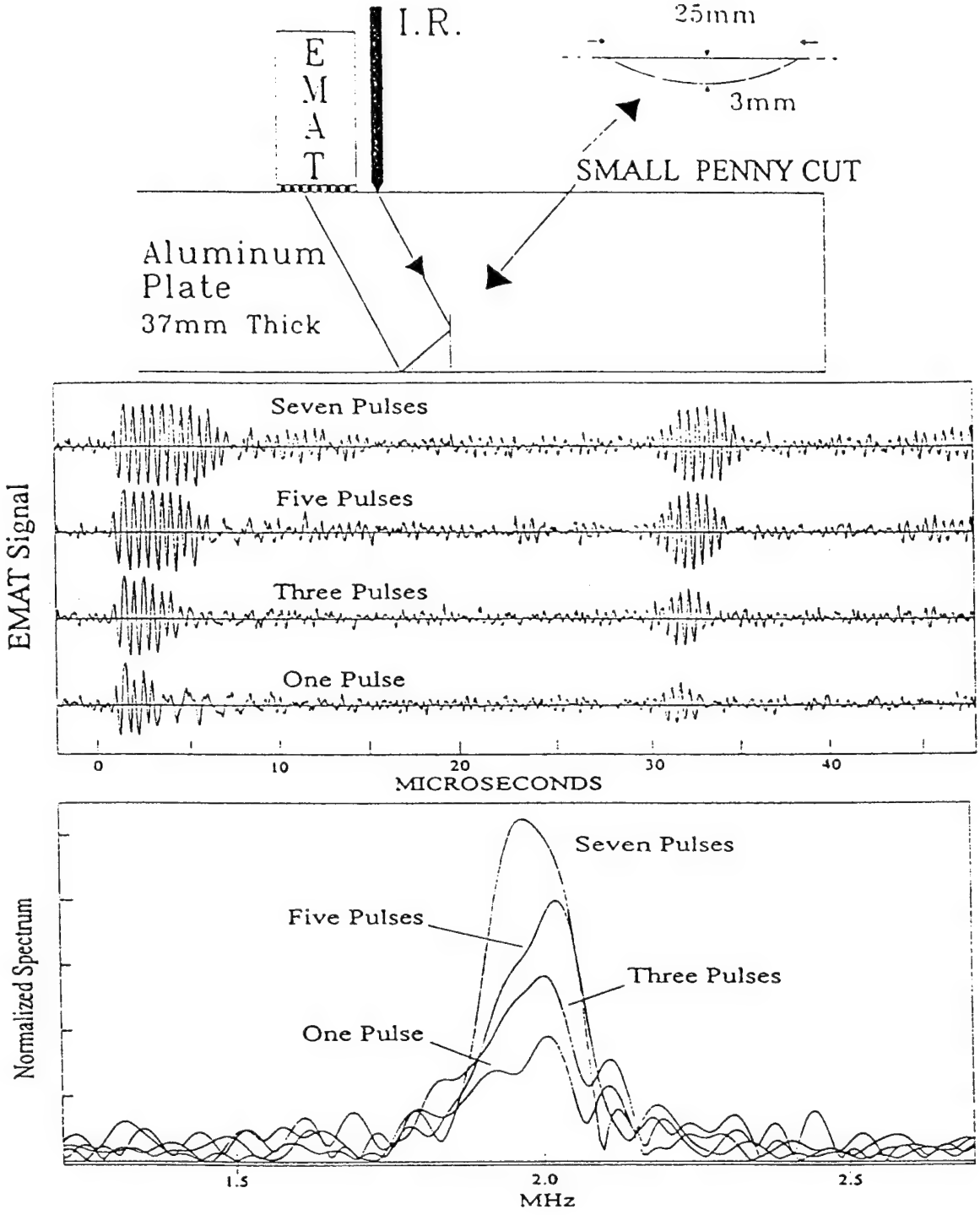

FIGURE 4. Multiple pulse laser excitation on ultrasound in an aluminum plate containing a penny shaped cut. The received EMAT signals are shown for one, three, five, and seven pulse sequences. The signal's normalized frequency spectrum is also shown.

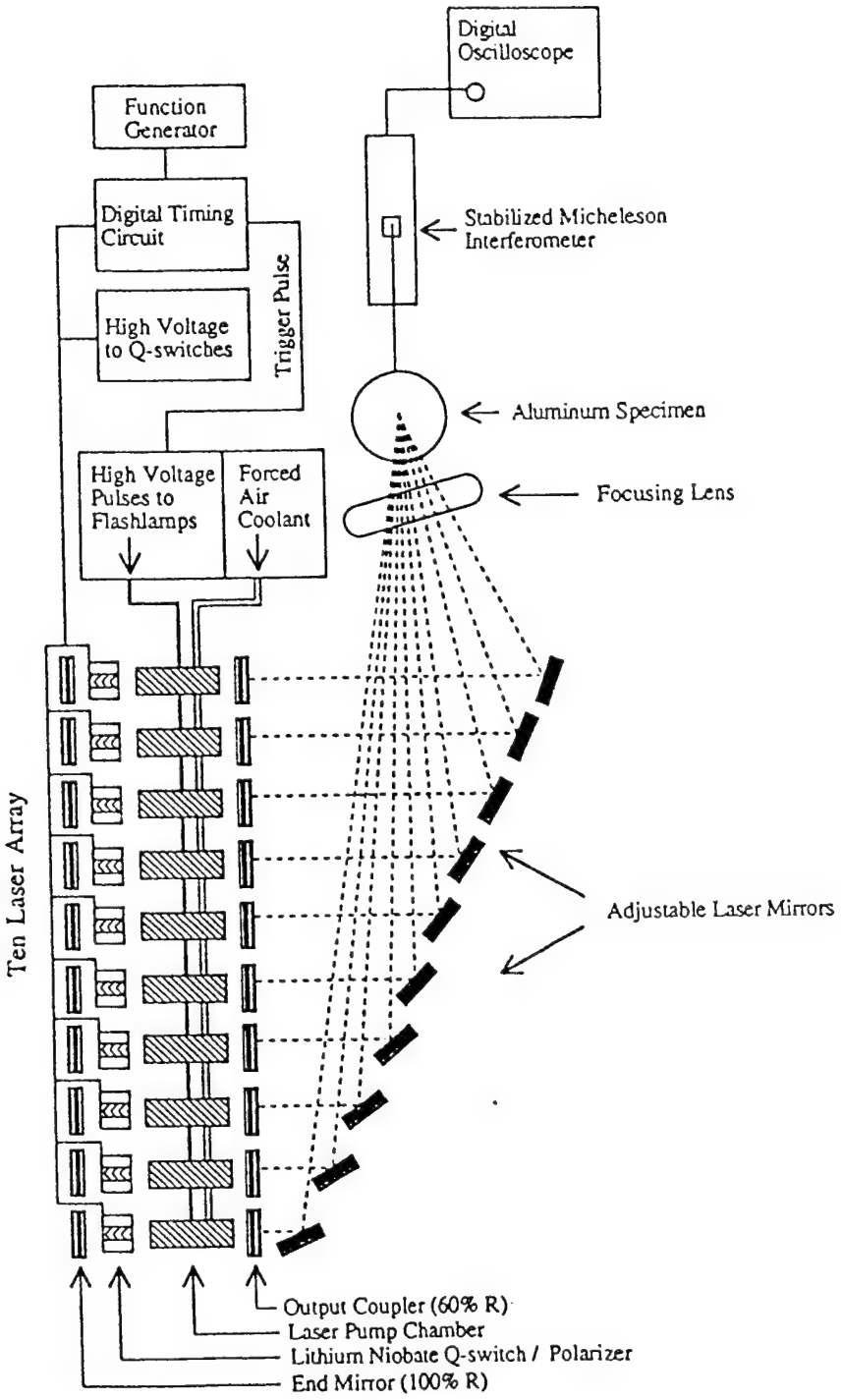

FIGURE 5. Schematic diagram of ten cavity Nd:YAG laser system for generation of narrow frequency band ultrasound and laser interferometer detection.

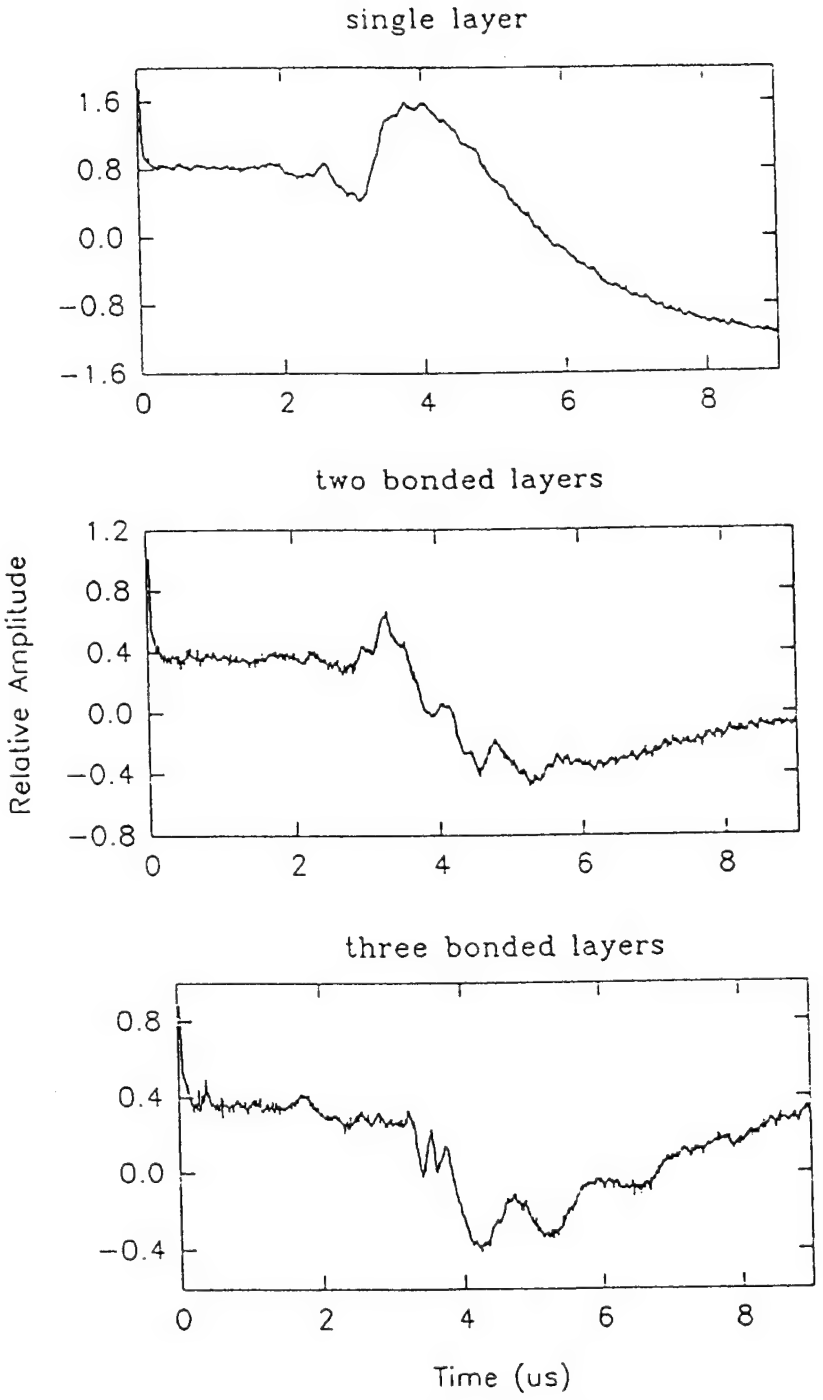

FIGURE 6. Experimental waveforms received from single pulse laser excitation of ultrasound in an aluminum lap joint made from 1 mm thick plates bonded with epoxy.
(a) waveform from a single plate
(b) waveform from two bonded plates
(c) waveform from three bonded plates

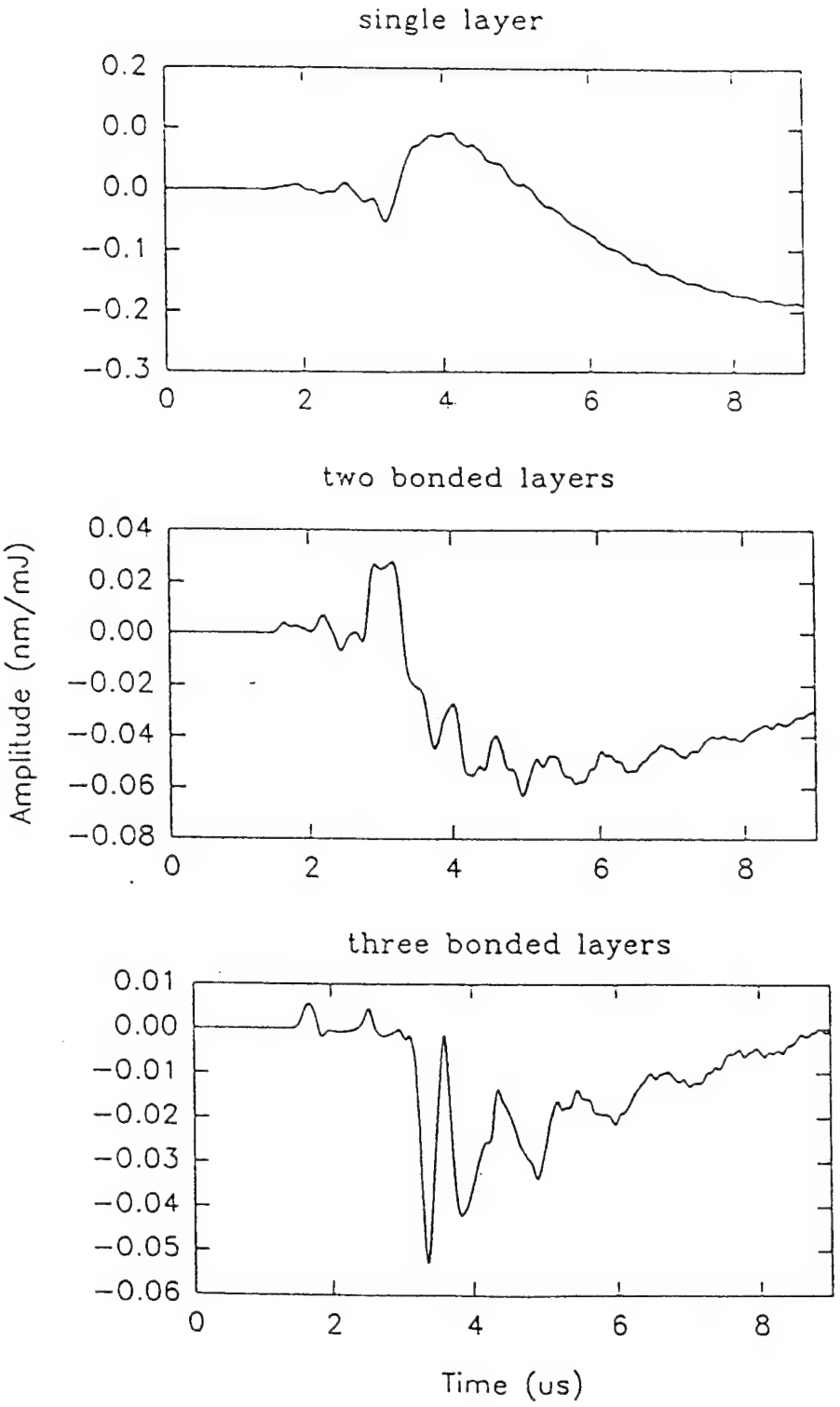

FIGURE 7. Theoretically predicted waveforms for single pulse laser generated/laser detected guided plate waveforms in 1, 2, and 3 mm thick aluminum plates. Effects of a finite bonding layer between plates have been neglected

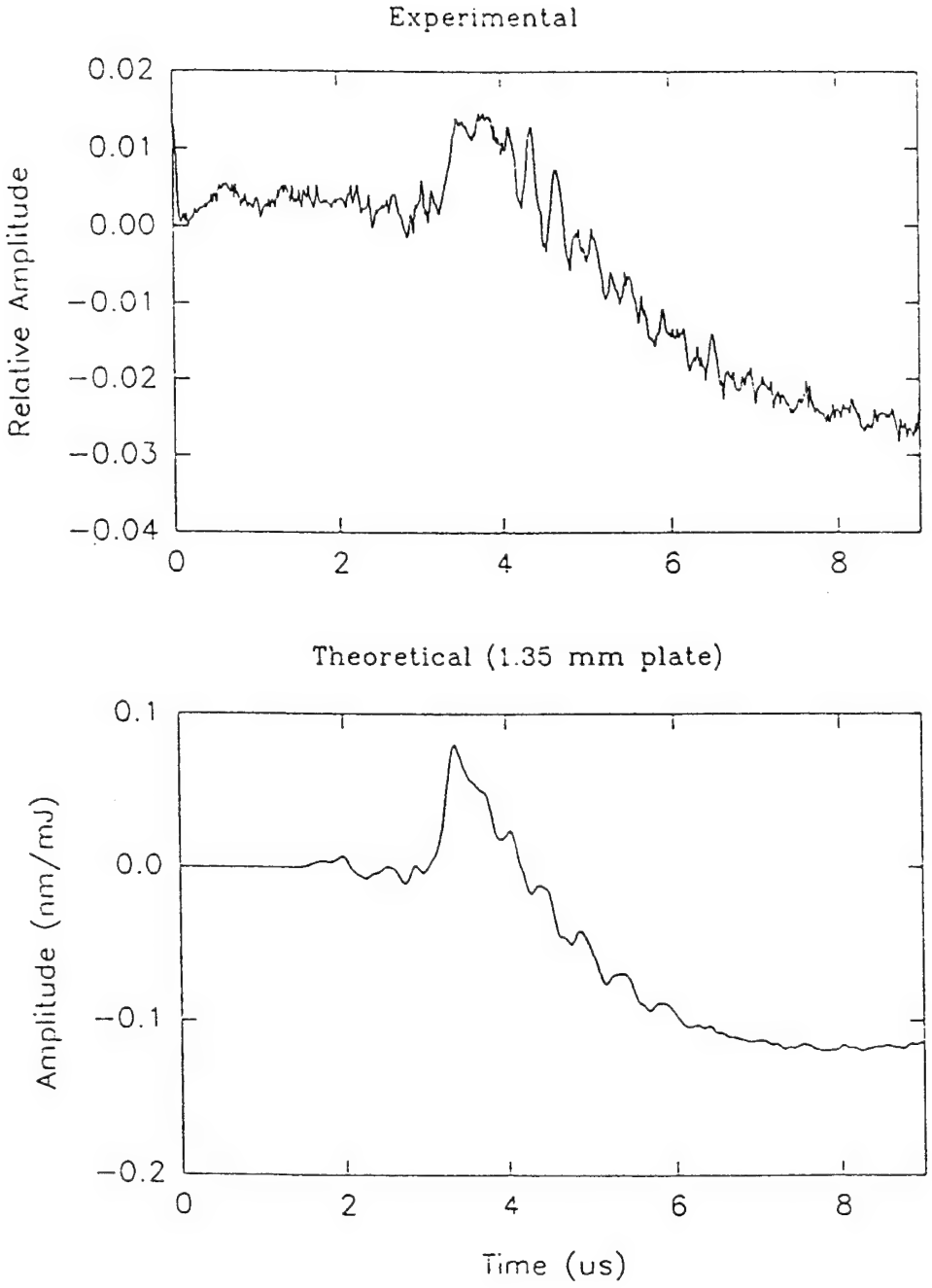

FIGURE 8. Laser generated/laser detected plate waves in actual aircraft lap joint specimen. Comparison with theoretical waveforms for a 1.35 mm thick aluminum plate indicates these waveforms are plate waves propagating in the top most layer of aluminum, possibly indicating incomplete bonding between layers.

FIGURE 9. (a) Experimental single laser pulse generated/laser detected through transmission waveform recorded from a portion of an actual aircraft lap joint single aluminum layer from which the paint was removed.

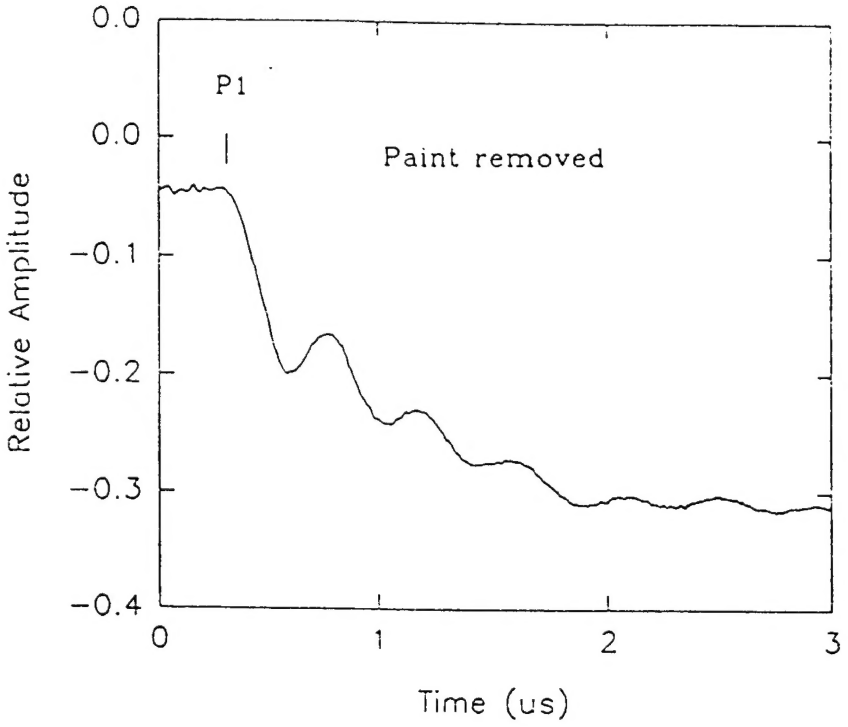

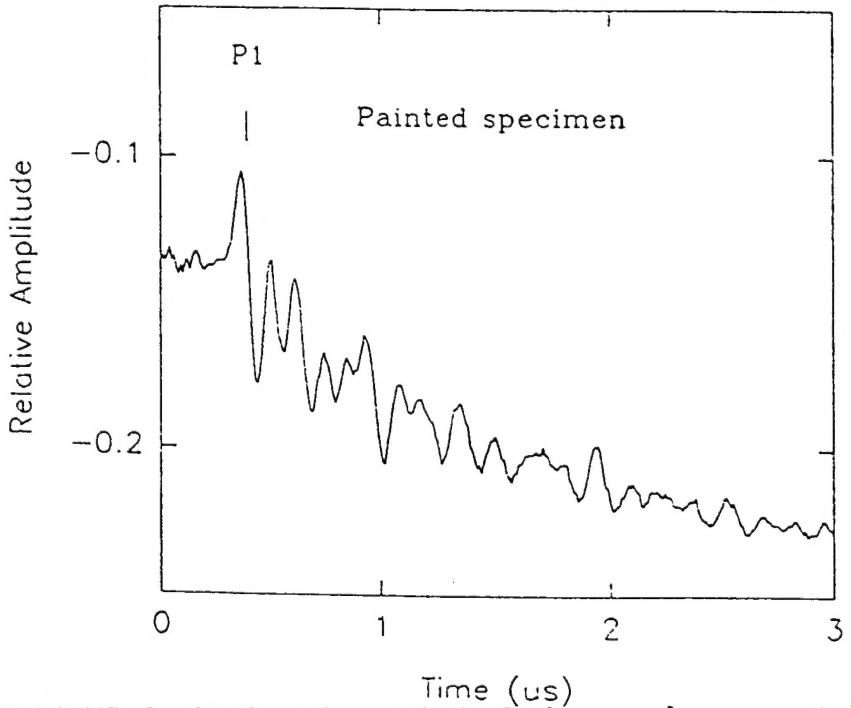

FIGURE 9. (b) Experimental single laser pulse generated/laser detected through transmission waveform recorded from a portion of an actual aircraft lap joint single aluminum layer which was painted

FIGURE 10. (a) Experimental single laser pulse generated/laser detected through thickness transmission measurement through a single layer of a painted actual aircraft lap joint single aluminum layer.

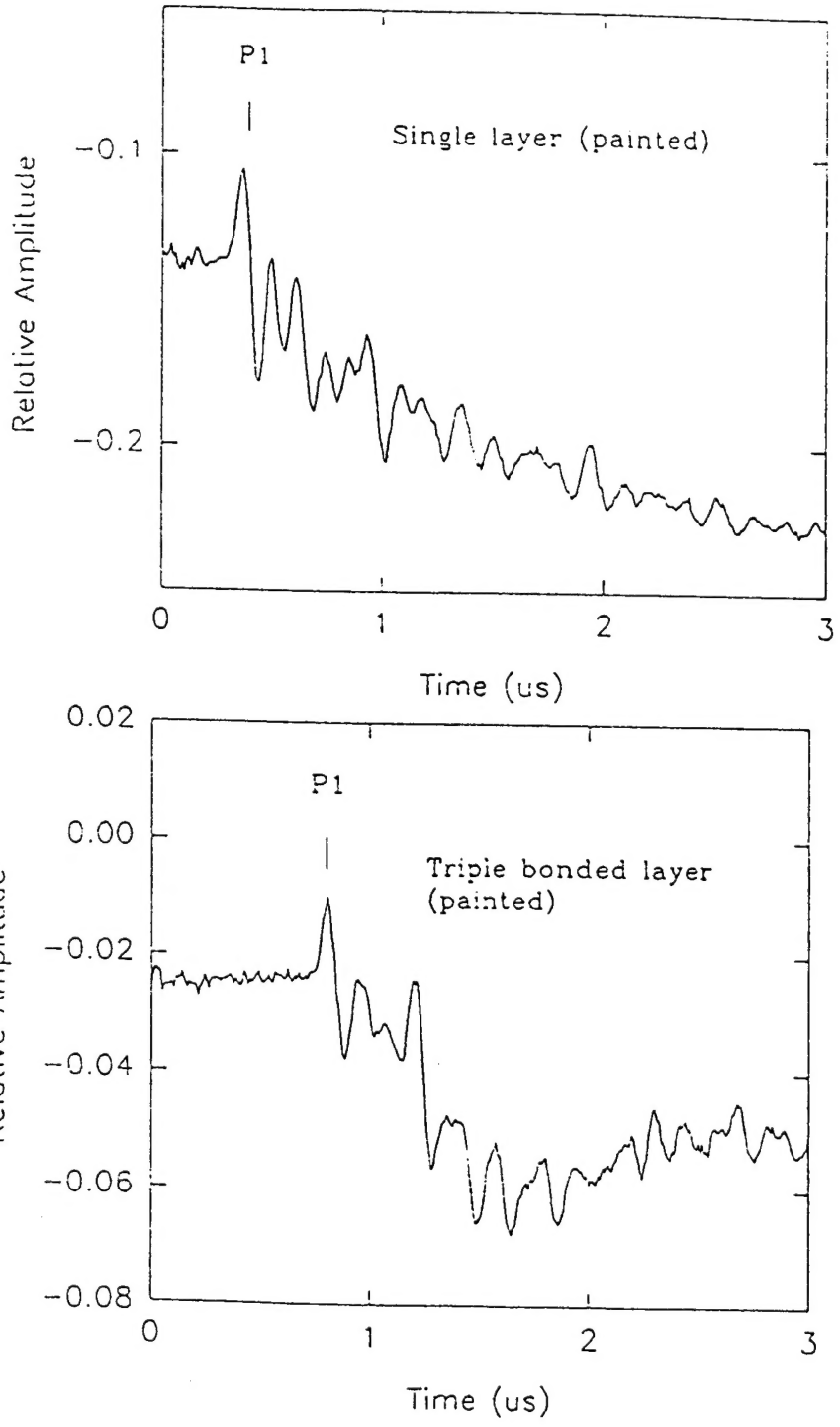

FIGURE 10. (b) Experimental single laser pulse generated/laser detected through thickness transmission measurement through a triple bonded layer of a painted actual aircraft aluminum lap joint.

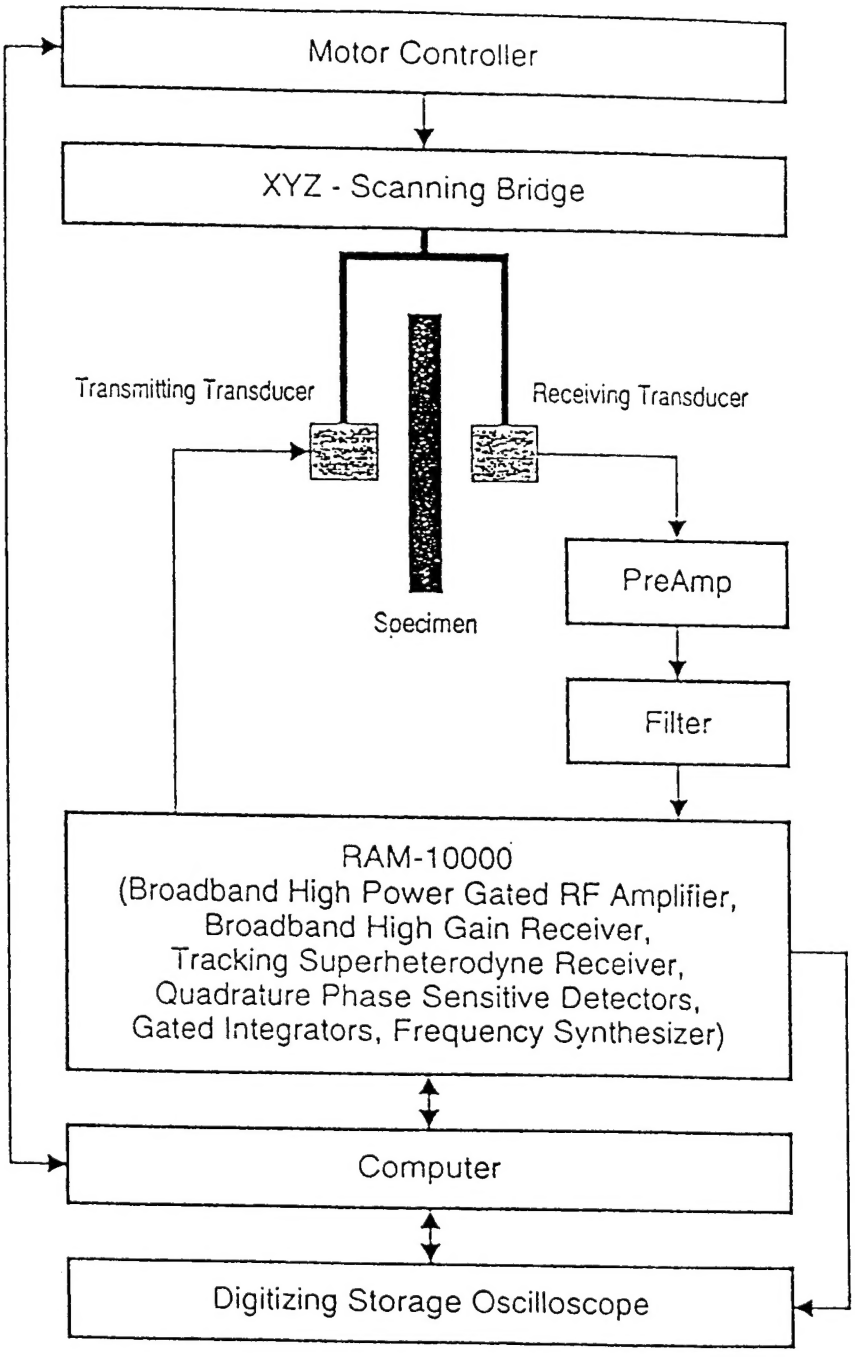

FIGURE 11. **Schematic drawing of the experimental arrangement for laser generation/air-coupled detection of ultrasound.**

Laser Ultrasonic C-Scan Results

Sample: 1.2" thick steel with 2.5" x 2.5" recesses milled in back surface (1/16", 1/8")

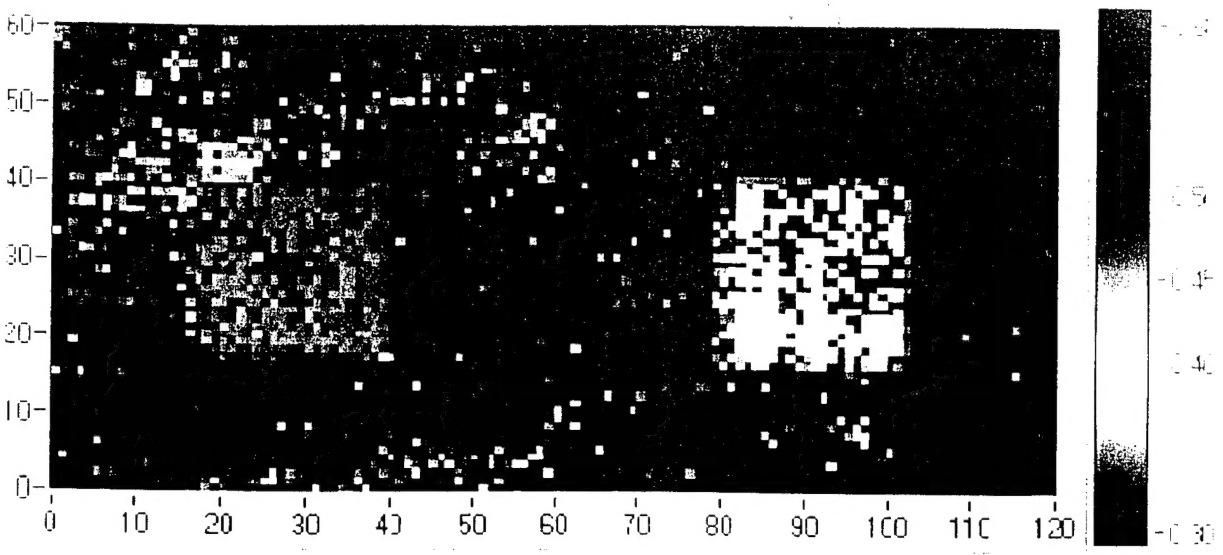

Sample: 1/2" thick steel with welds on back surface

Gating: Time-of-Flight

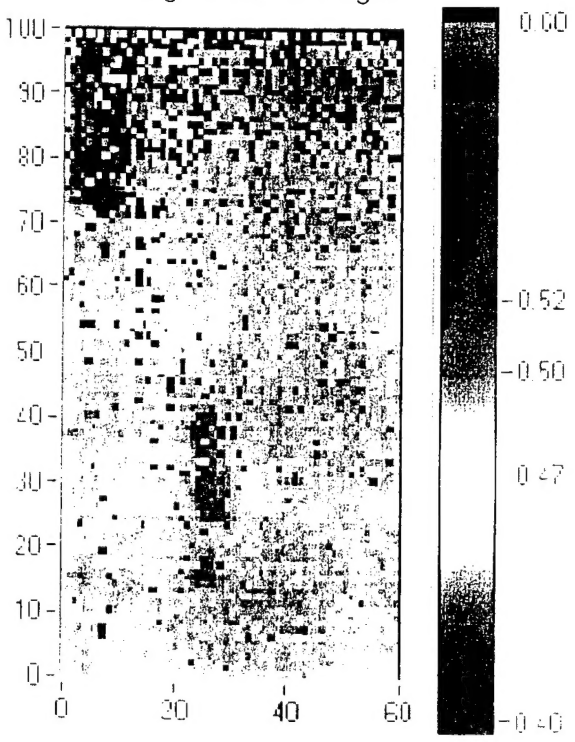

Gating: Amplitude